Triaryl-Like MONO-, BIS- and TRISKITPHOS Phosphines: Synthesis, Solution NMR Studies and a Comparison in Gold-Catalyzed Carbon-Heteroatom Bond Forming 5-*Exo*-Dig and 6-*Endo*-Dig Cyclizations

Simon Doherty,* Julian G. Knight,* Daniel O. Perry, Nicholas A. B. Ward, Dror M. Bittner, William McFarlane, Corinne Wills and Michael R. Probert

NUCAT, School of Chemistry, Bedson Building, Newcastle University, Newcastle upon Tyne, NE1 7RU, UK

ABSTRACT: A homologous series of triaryl-like KITPHOS-type monophosphines containing either one, two or three bulky 12-phenyl-9,10-dihydro-9,10-etheno-anthracene (KITPHOS) units have been developed and the influence of increasing steric bulk on their efficacy as ligands in gold(I)-catalyzed carbon-heteroatom bond-forming cyclizations investigated. Detailed solution NMR studies on Ph-TRISKITPHOS, its oxide and the corresponding gold(I)chloride adduct identified a conformational exchange process involving a concerted librational motion of the individual anthracene-derived organic substituents about their P-C bonds. The cessation of this motion at reduced temperatures lowers the molecular symmetry such that the two C_6H_4 rings in each of the KITPHOS units become inequivalent; a lower energy process involving restricted rotation of the biaryl-like phenyl ring has also been identified. Electrophilic gold(I) complexes of these triaryl-like KITPHOS monophosphines catalyze the 5-*exo*-dig cycloisomerization of propargyl amides to afford the corresponding methylene oxazolines which were used in a subsequent tandem carbonyl-ene reaction to afford functionalized 2-substituted oxazolines. A comparative survey revealed that catalyst efficiency for cycloisomerization decreases in the order MONOKITPHOS = BISKITPHOS > PPh_3 > TRISKITPHOS. The optimum system also catalyzes the selective 6-*endo*-dig cyclization of 2-alkynylbenzyl alcohols, 2-alkynylbenzoic acid and 2-(phenylethynyl) benzamides; gratifyingly, in several cases the yields obtained are markedly higher and/or reaction times significantly shorter than previously reported for related gold catalysts. Moreover, these are the first examples of gold(I)-catalyzed 6-*endo*-dig cycloisomerizations involving 2-(phenylethynyl) benzamides and, reassuringly, the optimum gold(I)/MONOKITPHOS systems either rivaled or outperformed existing silver or palladium-based catalysts. The steric parameters of this homologous series of phosphines have been quantified and compared with selected triarylphosphines using a combination of Solid-G calculations, to determine the percentage of the metal coordination sphere shielded by the phosphine (the G parameter), and Salerno molecular buried volume calculations (Samb*V*ca) to determine the percent buried volume (%V_{bur}); the corresponding Tolman cone angles have also been determined from correlations.

INTRODUCTION

Arguably, since their introduction bulky electron-rich biaryl monophosphines have evolved into one of the most powerful and versatile classes of ligand for transition metal catalyzed carbon-carbon and carbon-heteroatom based couplings and cyclizations.[1] The success of these ligands is often attributed to a combination of factors including: (i) their basicity, which promotes activation of challenging aryl chlorides,[2] (ii) their steric bulk, which favors formation of the active monophosphine $L_1Pd(0)$ as well as the product forming reductive elimination step,[3] (iii) the architecture of the biaryl motif which increases catalyst life time by stabilizing the low-coordinate active species through a weak metal-arene interaction[4] and, most recently, (iv) the breakthrough development of readily activated palladacycle precatalysts that generate the active monoligated LPd(0) species with remarkable efficiency under mild conditions.[5] As such the biaryl motif has been the lead template for the design of alternative systems based on biaryl-like units including *N*-arylpyrroles,[6] 2-phenylindole,[7] arylpyrazole,[8,9] bipyrazole[9] Dalphos[10] as well as the 2,3-dihydrobenzo[*d*][1,3]oxophosphole framework.[11] Despite the resounding success of this class of monophosphine, electron-deficient bulky triaryl and triaryl-like monophosphines have also been reported to form highly active catalysts for a host of platinum group metal catalyzed transformations. For example, ferrocenyl-based triarylphosphine **1**,[12] ortho dimesitylboryl-substituted triarylphosphine **2**,[13] indolyl-based triarylphosphine **3**[14] and a hexadimethylammonium-substituted triarylphosphine, Bn-Dendriphos,[15] (Chart 1) all form highly efficient catalysts for Suzuki-Miyaura cross-coupling that outperform their triphenylphosphine counterpart and in some cases even couple extremely challenging substrate combinations such as electron-rich aryl chlorides or sterically congested systems. In other examples, bowl-shaped triarylphosphine **5** accelerates the rhodium- and copper-catalyzed hydrosilylation of ketones and ketimines compared with the corresponding triphenylphosphine-based system,[16] electron-deficient biaryl monophosphines form markedly more catalysts than their electron-rich SPHOS counterpart for the palladium-catalyzed direct arylation of heterocycles,[17] morpholine-modified triarylphosphine **4** (Mor-DalPhos) outperforms its electron-rich counterpart in the palladium-

catalyzed α-arylation of acetone with electron-deficient electrophiles,[18] triaryl-based indolylphosphine **3** combines with $Pd_2(dba)_3$ to form a highly efficient catalyst for the borylation of aryl chlorides[19] and bulky triarylphosphines form highly efficient systems for the selective telomerization of 1,3-butadiene with methanol.[20] The obvious advantages associated with triaryl monophosphines compared with their electron-rich counterparts is greater air-stability, ease of synthesis and lower cost which would render them practical alternatives, provided competitive performance can be achieved. In this regard, these examples should encourage further investigations to explore and develop the use of bulky electron-deficient triaryl-type monophosphines in platinum group metal-catalyzed transformations.

We have also embraced the biaryl design concept and developed the biaryl-like KITPHOS class of monophosphine (Chart 1) which bears a close architectural similarity to Buchwald's biaryl monophosphines. Specifically, KITPHOS monophosphines comprise a PR_2 group connected to a C-C double bond, albeit as part of an anthracene-derived bicyclic framework, and a non-phosphine containing proximal aryl ring that can be systematically modified as it is introduced in the form of a 1-alkynylphosphine oxide.[21]

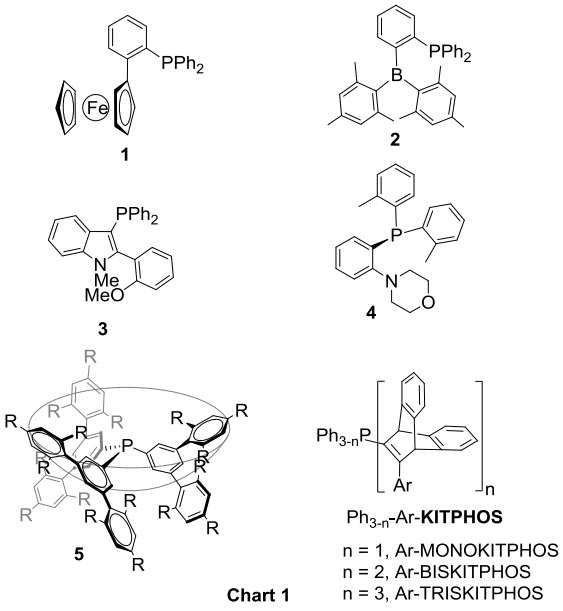

Chart 1

Not surprisingly, bulky electron-rich KITPHOS monophosphines are remarkably efficient ligands for a host of palladium-catalyzed carbon-carbon and carbon-nitrogen based cross-couplings[22] as well as gold-catalyzed intramolecular cyclizations.[23] Interested in exploring the extent to which diphenylphosphino-based KITPHOS monophosphines could be surrogates for conventional triarylphosphines we recently demonstrated that electron-deficient gold(I) complexes of diphenylphosphino-based KITPHOS monophosphines are markedly more efficient than their dicyclohexylphosphino counterparts for the 5-*exo*-dig cyclization of propargyl amides.[24] We have also shown that these phosphines can coordinate to ruthenium either in a conventional κ(P) manner or as κ(P):η^6 eight electron donors tethered through the proximal phenyl ring of the biaryl-like fragment to form constrained geometry complexes; both types of complex were shown to form efficient catalysts for the direct ortho arylation of 2-phenyl substituted *N*-heterocycles.[25] As Lewis acid gold(I) complexes of triphenylphosphine are often the catalyst of choice for cyclizations initiated by activation of a carbon-carbon multiple bond toward nucleophilic attack[26] we have pursued this analogy further and prepared an homologous series of triaryl-type KITPHOS monophosphines (Ph_{3-n}-Ar-KITPHOS; n = 1-3) and their corresponding gold(I) chloride complexes, undertaken comprehensive solution NMR studies to investigate an exchange process that lowers the molecular symmetry from C_{3v} to C_3, explored and quantified their steric properties and undertaken a comparative evaluation of their performance as catalysts for the cycloisomerization of propargyl amides, 2–(alkynyl)phenyl alcohols and 2–(phenylethynyl)benzamides with the aim of exploring the influence of increasing steric bulk on catalyst performance. The former substrates were selected as they are straightforward to prepare and routinely employed as benchmark substrates for comparing and evaluating the performance of new catalysts and the resulting alkylidene oxazolines are potentially useful synthons.[27] The latter two classes of substrate were chosen on the basis that the resulting isochromene and iminoisocoumarin motifs are present in a range of important therapeutic bioactive heterocycles,[28] but there is a clear need to identify more efficient systems as existing gold(I) catalysts are either limited by a poor substrate range and/or require long reaction times or high catalyst loadings due to low activity.[29] This study has demonstrated that catalysts based on triaryl-like MONOKITPHOS and BISKITPHOS monophosphines either outperform their triphenylphosphine counterpart, in some cases by quite some margin, or are markedly more efficient than the optimum reported system and are thus potential candidates for reaction development.

RESULTS AND DISCUSSION

Phosphine Synthesis and Gold(I) Coordination Chemistry. Having recently demonstrated that diphenylphosphino-based KITPHOS monophosphine **8a** outperforms its electron-rich dicyclohexylphosphino counterpart in the gold(I) catalyzed cyclization of methylene oxazolines,[24] we initiated a project to establish the influence on performance of increasing steric bulk within an homologous series of triaryl-like KITPHOS monophosphines by varying the number of attached anthracene-derived KITPHOS units. The phosphines required for this study were prepared in moderate to excellent yield following the procedure reported in our initial disclosure for the synthesis of **8a** (Scheme 1);[24] this involved a Diels-Alder cycloaddition between anthracene and the corresponding 1-alkynylphosphine oxide **6a-c**, to construct the bicyclic architecture of the KITPHOS framework, followed by reduction of the resulting monoxide **7a-c** either with chlorosilane/triethylamine in toluene (**7a-b**) or chlorosilane/tributylamine in xylenes (**7c**). The Diels-Alder reactions were most conveniently carried by heating the reactants in sealed 20 mL Wheaton V-20 reaction vials on an Asynt DrySyn multi-position heating block and using ^{31}P NMR spectroscopy to monitor the progress of reaction at regular intervals. The identity and purity of **8a-c** have been established by a combination of conventional spectroscopic and analytical techniques, full details of which are provided in the supporting information. With the aim of exploring the influence on catalyst efficiency of removing the proximal biaryl-like phenyl ring, **8d** was also prepared for comparative catalyst testing. The

ethynyldiphenylphosphine oxide required for the associated Diels-Alder cycloaddition step was prepared according to a previously reported method[30] and the desired phosphine oxide and corresponding phosphine were both isolated in high yield.

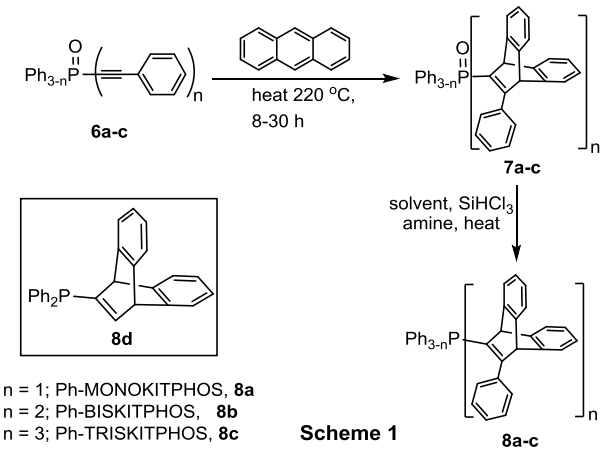

Scheme 1

Interestingly, the room temperature ^{1}H NMR spectrum of **7c** and **8c** both contain a combination of exchange-broadened resonances together with sharp well-resolved signals. The nature of this line-broadening was investigated further using a combination of variable temperature NMR studies including 2D EXSY and line-shape fitting, details of which are discussed in the following section. Even though the spectroscopic properties and analytical data for **7a**–**d** and **8a**–**d** are entirely consistent with their formulation, the exchange-broadened resonances in the ^{1}H NMR spectrum of **7c** and **8c** prompted us to undertake a single-crystal X-ray study of the former to compare key structural parameters with those of related triaryl-type monophosphine oxides; a perspective view of the molecular structure is shown in Figure 1.

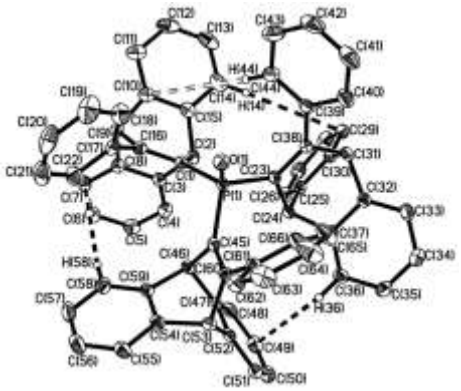

Figure 1 Molecular structure of 11-[tris(12-phenyl-9,10-dihydro-9,10-etheno-anthracene)]phosphine oxide (**7c**). Innocent hydrogen atoms and the dichloromethane molecules of crystallization have been omitted for clarity. Ellipsoids are at the 40% probability level.

The molecular structure clearly shows that the phosphorus atom is buried deep within a bowl-shaped cavity generated by a near C_3-symmetrical arrangement of the (*E*)-9-(1-phenylprop-1-en-1-yl)-9,10-dihydroanthracene units and that the proximal phenyl rings are directed towards the rim. A closer inspection of the structure reveals that one of the ortho protons of a C_6H_4 ring lies directly over and in close proximity (3.1-3.3 Å) to a C_6H_4 ring of an adjacent 12-phenyl-9,10-dihydro-9,10-etheno-anthracene unit; such a conformer would account for the high-field shifted aromatic signal in the low-temperature ^{1}H NMR spectrum of **7c**. The P-C bond lengths of 1.808(2)–1.811(2) Å are close to those in triphenylphosphine oxide (1.798(2)–1.802(2) Å) while the P-O bond length of 1.4745(14) Å is slightly shorter than that of 1.484(1) Å in the same molecule;[31] this shorter P-O bond length may also be responsible for the slightly larger average O-P-C angle of 114.08(9)° in **7c** compared with the corresponding angle of 112.25(6)° in $O{=}PPh_3$.

In order to undertake a comparative evaluation of the efficacy of triaryl-like KITPHOS monophosphines in gold-catalyzed cycloisomerizations the corresponding homologous series of gold(I) precatalysts LAuCl (**9b**–**d**) were prepared by reaction of [Au(2,2′-thiodiethanol)Cl][32] with the corresponding KITPHOS monophosphine, according to the procedure reported for the synthesis of **9a** (Equation 1);[24] in each case the product was purified by slow diffusion of a chloroform solution layered with methanol. Interestingly though, the extent of line-broadening is distinctly different to that for either **7c** or **8c**; this was confirmed with a variable temperature ^{1}H NMR study which identified two exchange processes in the accessible temperature range, the results of which are also described in detail in the following section.

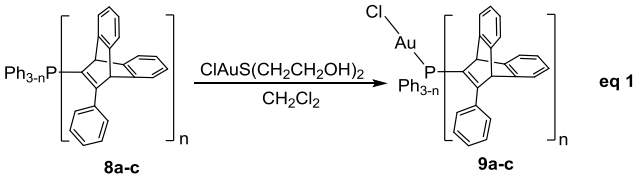

eq 1

As relatively few gold(I) complexes of KITPHOS monophosphines have been crystallographically characterized,[23a,24] single-crystal X-ray analyses of **9a-c** were undertaken; perspective views of the molecular structures are shown in Figures 2-4, respectively. In each case the geometry at the gold is close to linear and the P-Au-Cl bond angles of 174.78(7)° (**9a**), 177.88(3)° (**9b**) and 178.01(4)° (**9c**) lie well within the range reported for related complexes.[33] The Au-Cl bond lengths of 2.2814(7) Å (**9a**), 2.2859(8) Å (**9b**) and 2.2921(9) Å (**9c**) are also similar to those in the six literature reported structures of PPh_3AuCl,[34,35] as are the Au-P bond lengths that range between 2.222(7) Å and 2.2308(8) Å. Interestingly, the 12-phenyl-9,10-dihydro-9,10-etheno-anthracene units of the TRISKITPHOS monophosphine in **9c** retain a near C_3-symmetrical arrangement with the gold center buried in the cavity formed by the proximal phenyl rings. Figure 4 also shows that one ortho proton on each 12-phenyl-9,10-dihydro-9,10-etheno-anthracene unit lies in close proximity to a C_6H_4 ring (C-H---aromatic distances between 2.6 and 3.4 Å) of a neighboring unit in much the same manner as described for **7c**, which would account for the similarity in their variable temperature ^{1}H NMR properties and the presence of the anomalously high-field shifted signal at δ 5.44 (*vide infra*). In addition, one of the ortho protons of each C_6H_5 ring is also orientated close to a C_6H_4 ring e.g. C(3)----H(40) = 2.765(3) Å; such an interaction is likely to be the cause of the sharp high-field signal at δ 6.16. There are also weak η^1-interactions

between the gold atom and the ipso carbon atoms of two of the flanking proximal phenyl rings in **9c**; the Au----C(17) and Au----C(39) distances of 3.195(3) Å and 3.219(3) Å, respectively, are both less than the sum of the van der Waals radii of gold and carbon and the former is similar to the Au----C_{ispo} interactions reported for gold(I) chloride complexes of PCy_2(*o*-biphenyl) and PBu^t_2(o-biphenyl).[36] In contrast, a weak interaction between the gold and the π-face of the remaining proximal phenyl ring involves C_{ortho} and the distance of 3.195(3) Å is markedly shorter than the corresponding Au----C_{ipso} distance of 3.344(3) Å. In comparison, there are no significant η^1-interactions between the π-face of the proximal phenyl rings and gold in **9a** and **9b**; the shortest Au----C contacts within these molecules are 3.328(3) Å (Au----C_{ipso}) and 3.317(4) Å (Au----C_{ortho}), respectively. As **9d** lacks a proximal phenyl ring and belongs to the triaryl-like class of monophosphine, a single-crystal X-ray structure determination was also undertaken to provide additional data for use in quantifying the steric parameters of these phosphines; a perspective view of the molecular structure is shown in Figure 5. Interestingly, the P-Au-Cl angle of 172.01(3)° shows a much larger deviation from linearity than **9a-c** while the rigid framework of the anthracene-derived unit prevents formation of an Au----C_6H_4 interaction.

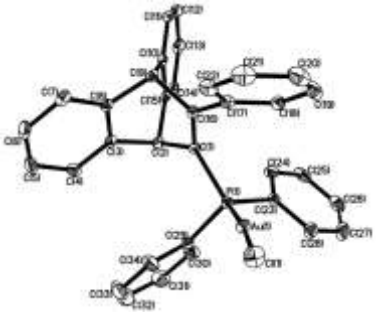

Figure 2 Molecular structure of 11-(diphenylphosphino)-12-phenyl-9,10-dihydro-9,10-ethenoanthracene gold(I) chloride (**9a**). Hydrogen atoms and the chloroform molecule of crystallization have been omitted for clarity. Ellipsoids are at the 40% probability level.

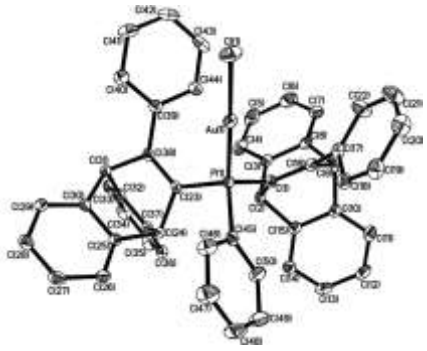

Figure 3 Molecular structure of 11-[bis(12-phenyl-9,10-dihydro-9,10-etheno-anthracene)]phenylphosphine gold(I) chloride (**9b**). Hydrogen atoms and the chloroform molecule of crystallization have been omitted for clarity. Ellipsoids are at the 40% probability level.

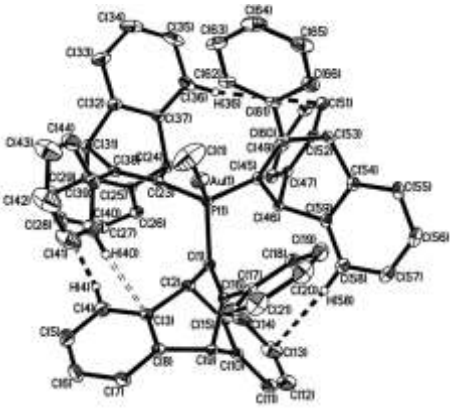

Figure 4 Molecular structure of 11-[tris(12-phenyl-9,10-dihydro-9,10-etheno-anthracene)]phenylphosphine gold(I) chloride (**9c**). Innocent hydrogen atoms and the chloroform and methanol molecules of crystallization have been omitted for clarity. Ellipsoids are at the 40% probability level.

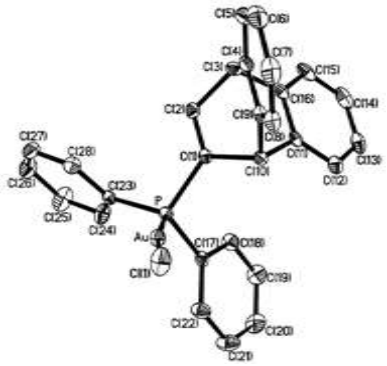

Figure 5 Molecular structure of [11-(diphenylphosphino)-9,10-dihydro-9,10-ethenoanthracene] gold(I) chloride (**9d**). Hydrogen atoms and the chloroform molecule of crystallization has been omitted for clarity. Ellipsoids are at the 40% probability level.

Solution State NMR studies of 7c, 8c and 9c. Comparative NMR studies of these three molecules show that they have very similar patterns of proton and carbon chemical shifts and coupling constants (Tables S1 and S2 of the supporting information) that are fully consistent with their proposed structures. Hindered rotation about the P–C bonds produces a propeller-like configuration which leads to inequivalence of the two C_6H_4 rings in each substituent and the corresponding numbering scheme is shown below in Figure 6. In all three compounds exchange behavior leads to spectra with combinations of sharp and broad lines, and the various spectra differ markedly in appearance from compound to compound at any given temperature, even though most of the corresponding chemical shifts and coupling constants do not differ greatly. Detailed NMR studies including 2D-EXSY and line-shape fitting were therefore undertaken over the temperature range 165–400 K in $CDCl_3$, CD_2Cl_2 and *o*-$C_6D_4(CD_3)_2$ in order to elucidate the exact nature of the dynamic behavior.

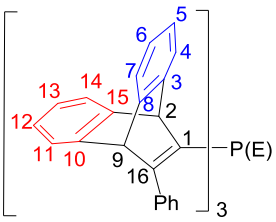

Figure 6 Compound **7c** (E = O), **8c** (E = electron lone pair), **9c** (E = Au – Cl). For the phenyl groups the atom numberings are 17 (*ipso*), 18, 22 (*ortho*), 19, 21 (*meta*) and 20 (*para*). In the second and third substituents of phosphorus the positions are designated 1′, 2′…. and 1″, 2″…. respectively.

Over the entire temperature range the proton-decoupled ^{31}P spectrum for each compound remained a single sharp line ($\nu_{½}$ < 2 Hz) at δ 18.6, –24.8, and 5.6 for **7c**, **8c** and **9c**, respectively, confirming that the exchange is intramolecular. The proton and ^{13}C spectra can be interpreted on the basis of the above structure which is essentially static at very low temperatures. A complete and unequivocal spectroscopic assignment was achieved using a combination of COSY, NOESY, ROESY, HSQC and HMBC 2D spectra together with ^{1}H–{^{31}P} decoupling and comparisons of ^{13}C spectra obtained at 125 and 175 MHz to identify ^{31}P–^{13}C splittings. All spectra were consistent with the three individual anthracene-derived organic substituents of phosphorus remaining fully equivalent throughout the exchange activity.

Two distinct exchange processes were identified: (i) concerted hindered rotation of each phenyl ring about its C_{16}–C_{17} (*ipso*) axis associated with inequivalence of its two *ortho* and of its two *meta* positions in the proton and ^{13}C spectra; and (ii) concerted librational motion of the individual organic substituents about their P–C_1 bonds associated with the 3/15, 4/14, 5/13, 6/12, 7/11, and 8/10 equivalences at higher temperatures. Figure 7 shows a series of proton NMR spectra of compound **9c** in the range 175 to 230 K which clearly illustrates the restricted rotation of its phenyl groups. Corresponding behavior was shown by the *ortho* and m*eta* ^{13}C resonances while the *para* proton and *para* and *ipso* ^{13}C signals remained sharp at all temperatures. Simulations using the program gNMR gave excellent fits for those *ortho* and *meta* proton resonances which were not overlapped by other signals, and application of the Eyring equation yielded $\Delta H^{‡}$ = 37.9 kJ mol^{-1} and $\Delta S^{‡}$ = –4.4 J mol^{-1} K^{-1}. Only in the case of the gold complex **9c** were the energetics suitable for obtaining thermodynamic data for both exchange processes in the accessible temperature range (165 to 400 K) and therefore the majority of the discussion will concentrate on this species. For **7c** and **8c** rotation of the phenyl rings was still comparatively rapid at 165 K, although line-broadening of the *ortho* and *meta* resonances at this temperature made apparent the onset of restricted rotation. It thus appears that the extent of internal steric congestion is significantly greater in **9c** than in **7c** or **8c**.

For **9c** the crystal structure (*vide supra*) shows that in the solid state the three organic substituents of phosphorus are very nearly equivalent, although a propeller twist renders the molecule chiral and reduces the symmetry from C_{3v} to a close approximation to C_3 as shown in Figure 8. An estimate of the deviation from a true threefold axis is provided by the three dihedral angles Au/P/C_1/C_{16}, Au/P/$C_{1'}$/$C_{16'}$ and Au/P/$C_{1''}$/$C_{16''}$ which are 22.65º, 22.6º and 20.7º, respectively. Thus, concerted librations of *ca.* 44º about the corresponding P–C_1 sub-axes are sufficient to interconvert the enantiomers and remove the inequivalences 3/15 etc. as also shown in Figure 8. It is clear that this is the process (ii) observed in the proton and ^{13}C spectra at higher temperatures, and there is no need to postulate complete freedom of rotation about the P–C_1 etc. bonds.

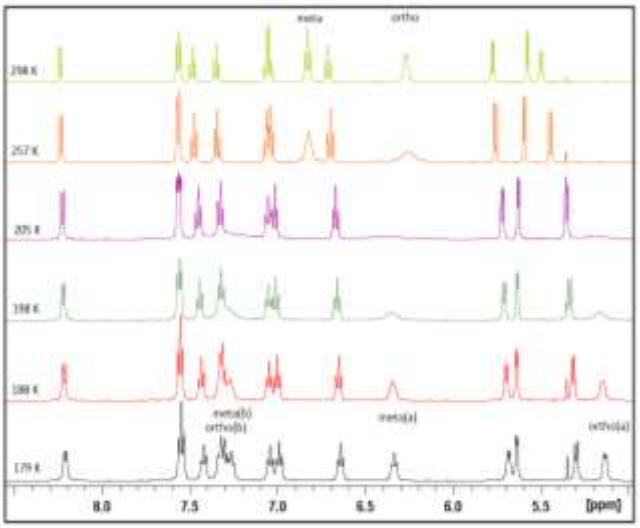

Figure 7 Variable temperature ^{1}H NMR spectra for gold complex **9c** showing restricted rotation of phenyl groups; spectra were recorded in CD_2Cl_2 at 500 MHz**.**

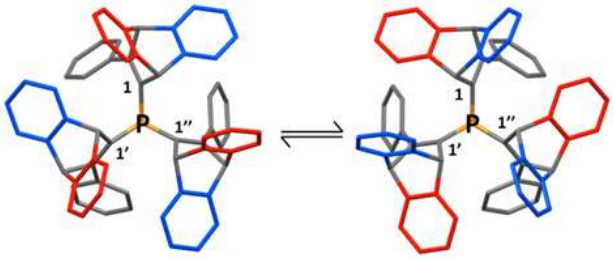

Figure 8 Views down P–Au bond in **9c** (C_3 axis) showing interchange of environments of red and blue C_6H_4 rings as a result of concerted *ca.* 44 deg. rotations of each substituent about the P–C_1, P–$C_{1'}$ and P–$C_{1''}$ bonds.

A striking feature of the proton data for **9c** is the large chemical shift difference between the two *ortho* (and to a lesser extent the two *meta*) protons of the phenyl groups. This can be attributed to the exposure of one of the ortho protons to the axial component of the diamagnetic anisotropy (ring current) of one of the aromatic C_6H_4 rings in a different substituent. For example, H18′ would be exposed to ring A as shown in Figure 9, whereas its counterpart in the same ring (H22′) would not be so influenced. An approximate calculation based on the tables of Johnson and Bovey[37] suggests that H18′ would be shielded by 1.9 ppm by this effect, although the good agreement with the observed chemical shift of δ = 5.2 ppm may well be fortuitous. In **7c**, **8c** and **9c** the large chemical shift difference between H4 and H14 is also noteworthy, and large shielding of the latter can

be similarly attributed to exposure to the axial ring current of ring B', i.e. the other C_6H_4 ring of a different substituent. The corresponding ^{13}C chemical shift differences are generally smaller, which is consistent with their being due to localized magnetic field rather than electronic effects.

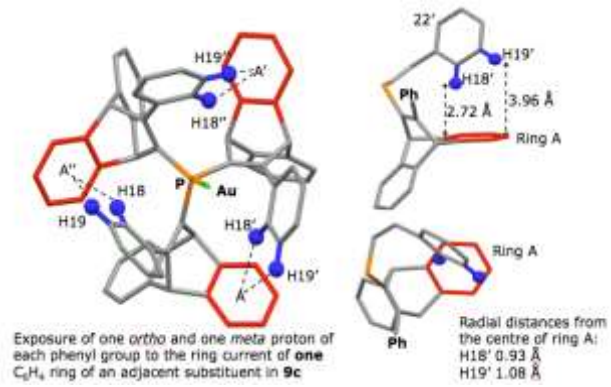

Figure 9 Perspective view of **9c** showing exposure of one of the *ortho* protons to the axial component of the diamagnetic anisotropy and views showing the details of this interaction and the radial distance from the centre of ring A.

From band-shape analysis of proton spectra using the program gNMR, together with intensities of off-diagonal peaks in 2D EXSY spectra for some slower rates, the exchange rates for process (ii) were determined for **7c**, **8c** and **9c** over a range of temperatures, and the corresponding Eyring plots are reproduced in Figure 10. The respective values of $\Delta H^{\ddagger}$ are 52.1, 66.3, and 75.4 kJ mol^{-1}, and those of $\Delta S^{\ddagger}$ are –26.5, –31.5, and –15.6 J mol^{-1} K^{-1}. The negative entropies of activation are consistent with a more ordered excited state, which is to be expected for a concerted process, and in which the Au/P/C_1/C_{16} dihedral angles are close to zero. The overall pattern of the free energies of excitation is perhaps not what would have been expected, and the following points should be noted.

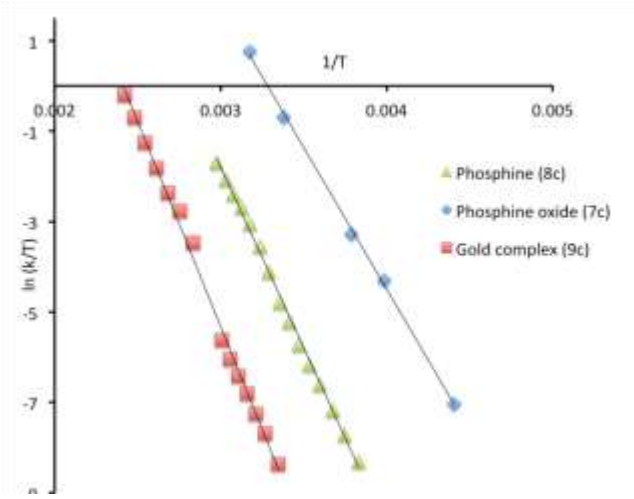

Figure 10 Eyring plots for the librational motion in **7c**, **8c**, and **9c** based on the exchange of H_4 and H_{14}.

The mean C-P-C interbond angles in **7c** and **9c** are 104.5 and 104.9 degrees, respectively, and although the value for **8c** is unfortunately not available it may be expected to be somewhat less. On this basis it is difficult to understand the order of the excitation energies found above, but it should be borne in mind that the extent of crowding in these species will affect the energies of both the ground and upper conformational states for the librational motion. An alternative measure of the internal congestion is provided by the E/P/C_1/C_{16} etc dihedral angles already mentioned. For **7c** the mean value is 28.0° and for **9c** it is 22.0° implying a capacity for less crowding in the former. Furthermore, the spread of the individual dihedral angles among the three substituents is much greater in **7c** (± 6.4°) than in **9c** (± 1.0°), which is again consistent with less congestion in the former.

A proton 500 MHz ROESY spectrum with a mixing time of 200 ms was obtained on **9c** in CD_2Cl_2 at 169 K and is shown in Figure 11. In addition to the negative (red) off-diagonal n.o.e. signals there are four positive (blue) off-diagonal signals arising from the slow chemical exchanges H_{18}/H_{22} (*ortho*) and H_{19}/H_{21} (*meta*) when the phenyl group rotates. This exchange also affects the intensities of n.o.e. signals involving these protons. The strongest n.o.e. interactions are, as expected, those within the same substituent between mutually *ortho* C_6H_4 protons, such as H_4/H_5 and H_5/H_6, and H_{18}/H_{19} in the phenyl groups. These are all associated with interatomic distances of *ca.* 2.5 Å. In the solid the three *endo* bridgehead protons H_2 etc. are only 2.7 Å apart and so should have significant mutual n.o.e. interactions, although their equivalence in solution makes these unobservable. Nonetheless, the mutual relaxation of these protons is affected and thus n.o.e. interactions with other protons are diminished, as is well known for the protons of methyl groups.

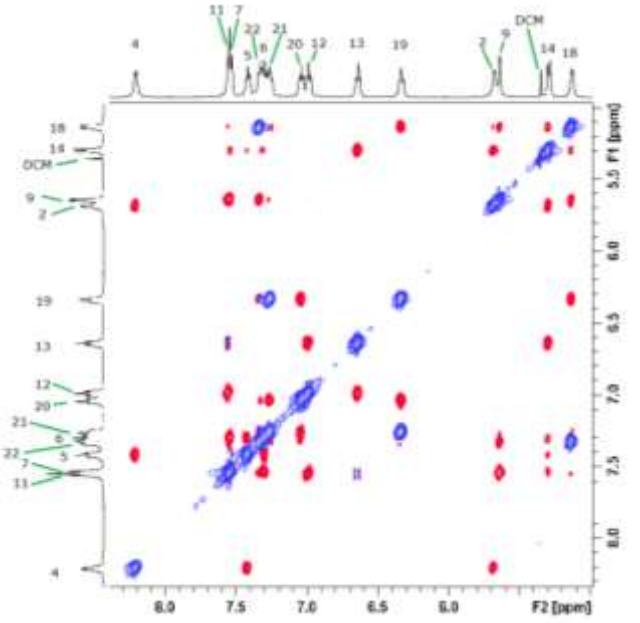

Figure 11 500 MHz ROESY NMR spectrum of **9c** in CD_2Cl_2 at 169 K with a mixing time 200 ms. Off-diagonal NOE peaks are red, off-diagonal exchange peaks are blue.

Of special importance are the apparent weak n.o.e. interactions of H_{14} with H_5, H_6 and H_7. However, the relevant interatomic distances are 5.46, 7.29 and 6.54 Å, respectively, all too great for there to be any significant n.o.e. interaction. We

therefore attribute these observed off-diagonal signals to interaction of H_{14} with $H_{5'}$, $H_{6'}$ and $H_{7'}$ (in the other portion of a different substituent) for which the respective distances are 3.96, 3.97 and 3.82 Å and this serves to confirm the close similarity of the structures in the solid state and in solution. It is noteworthy that for the counterpart of H_{14}, i.e. H_4, the corresponding intra-substituent distances are of course essentially the same, but owing to the propeller twist of the molecule the inter-substituent distances to $H_{11''}$, $H_{12''}$ and $H_{13''}$ are much greater, *viz.* 7.64, 7.50 and 5.81 Å. Thus, no corresponding n.o.e interactions are seen, which is again fully consistent with comparability of the solution and solid state structures. It is also worth noting that in the case of potential H_4/H_{14} etc. interactions some relevant distances are H_4/H_{14} = 4.50 Å, $H_{4'}/H_{14}$ = 3.86 Å, and $H_4/H_{14''}$ = 3.47 Å, any of which could in principle generate a significant n.o.e. However, in practice this will be cancelled by slow residual H_4/H_{14} exchange which is still occurring at 169 K. In view of the high level of internal congestion in these molecules there is little opportunity for significant internal motions, so it is indeed to be expected that the solid and solution-state structures will be very similar.

Steric Properties of Triaryl-like KITPHOS Monophosphines: A Comparison with Triarylphosphines. The steric properties of bulky triaryl and triaryl-like phosphines have been suggested to be integral to their efficacy as ligands in a host of platinum group metal-catalyzed transformations[1] and gold-catalyzed inter- and intramolecular additions to carbon-carbon multiple bonds.[38] As the steric bulk of the triaryl-like KITPHOS class of monophosphine can be modified in a systematic manner and, interested in identifying applications of this class of phosphine in catalysis, we have attempted to quantify their steric properties using the percent buried volume ($\%V_{bur}$) model and Solid-G calculations in order to compare with their more common triarylphosphine counterparts. The percent buried volume model was introduced by Nolan and Cavello[39] to overcome the limitations of the Tolman model[40] which can be either inadequate or ineffective for calculating the steric parameters of *N*-heterocyclic carbenes and phosphines with structurally elaborate architecture; it was designed to better define the steric pressure brought about by these ligands. In this model, the percent buried volume is defined as the percent of the total volume of a sphere occupied by a ligand and is calculated using the Samb*V*ca software.[41] As there is an excellent correlation between the steric properties quantified by the Tolman cone angle and the percent buried volume values calculated from crystal structure data on gold(I) complexes of the type [PR_3AuCl], the percent buried volumes for **9a-d** have been determined to compare with the corresponding values for selected gold(I) complexes of conventional triarylphosphines, full details of which are presented in Table 1. The $\%V_{bur}$ value of 32.3 determined for **9a** is close to that of 29.9 for PPh_3AuCl, while BISKITPHOS is significantly larger and the $\%V_{bur}$ of 47.4 is closer to that of 45.0 for trimesitylphosphine and 43.6 for 2,4,6-$((MeO)_3C_6H_2)_3P$ (entries 6 and 7); other common triarylphosphines including $PPh(anthracenyl)_2$, P(*o*-tolyl)$_3$ and $P(C_6F_5)_3$ have intermediate $\%V_{bur}$ values (entries 9-11). In comparison, the $\%V_{bur}$ value of 64.5 for TRISKITPHOS in **9c** is among the largest to be documented and bigger than that of 58.7 for $P(SiMe_2{}^tBu)_3$, (entry 12) which does not form metal-based coordination complexes. The anomalously large $\%V_{bur}$ value for **9c** may be reconciled by appreciating that the gold atom sits deep within a bowl-shaped cavity formed by a near C_3-symmetric arrangement of bicyclic anthracene-derived KITPHOS fragments with the proximal aryl rings projecting towards the rim. A qualitative estimate of the steric contribution provided by the proximal phenyl ring in KITPHOS monophosphines can obtained by comparing the $\%V_{bur}$ of 32.3 for **9a** with that of 28.9 for **9d** which corresponds to a 3.4% increase in the buried volume; the latter value is similar to that of 29.9 calculated for PPh_3AuCl. In comparison, we have previously commented that the corresponding difference between PCy_2Ph and Cy-JohnPhos in [LAuCl] provides a measure of the steric influence of the proximal phenyl ring in dicyclohexyl-based arylphosphines; in this case the $\%V_{bur}$ values of 32.7 and 46.7, respectively, correspond to an increase in the buried volume by 14%. Similarly, a measure of the steric influence on the introduction a single *o*-phenyl ring into triphenylphosphine can be obtained from the $\%V_{bur}$ values of 29.9 and 42.6 for PPh_3AuCl and [PPh_2(o-biphenyl)AuCl], respectively; this increase in buried volume of 12.7% aligns with the increase of 14% from PCy_2Ph to [JohnPhosAuCl]. Interestingly, the increase in $\%V_{bur}$ of 3.4 that results from introducing a proximal *o*-phenyl ring into **8d** is much smaller than the corresponding increase for PCy_2Ph and PPh_3 which supports our earlier observation that KITPHOS monophosphines appear to be sterically malleable and capable of adjusting their bulk according to the immediate surroundings; i.e. the space available around the metal centre. Thus, there appear to be subtle differences in the factors that influence the steric bulk of KITPHOS monophosphines compared with their biaryl counterparts which may well be manifested in their performance as ligands for catalysis.

Table 1. $\%V_{bur}$ Values and Cone Angles Calculated for KITPHOS Monophosphines and Selected Triarylphosphines in [LAuCl]

entry	complex	$\%V_{bur}$[a]	cone angle θ/deg
1	Ph-MONOKITPHOSAuCl	32.3	156[b]
2	Ph-BISKITPHOSAuCl	47.4	229[b]
3	Ph-TRISKITPHOSAuCl	64.5	310[b]
4	MONOKITPHOSAuCl	28.9	140[b]
5	PPh_2(*o*-biphenyl)AuCl	42.6	206[b]
6	$PMes_3$AuCl[42]	45.0	212
7	$P(2,4,6\text{-}(OMe)_3C_6H_2)_3$AuCl[43]	43.6	211
8	PPh_3AuCl[35]	29.9	145
9	P(*o*-tol)$_3$AuCl[44]	39.4	194
10	$P(C_6F_5)_3$AuCl[45]	37.3	184
11	$PPh(9\text{-anthracenyl})_2$AuCl[46]	38.9	188
12	$P(SiMe_2{}^tBu)_3$[47]	58.7	-

[a] $\%V_{bur}$ for Au-P bond length at 2.28 Å. [b] Calculated by linear regression.

The steric parameters for selected triaryl-like KITPHOS monophosphines and triarylphosphines relevant to this study have also been determined using Solid-G calculations, details of which are listed in Table 2. This

approach provides a measure of the steric congestion in terms of the percentage of the metal coordination sphere shielded by the ligand; quantitatively, the G parameter provides a measure of the probability of an incoming reagent NOT accessing the meal centre.[48] The G parameters for the homologous series of phenyl-substituted KITPHOS monophosphines increases steadily with increasing number of anthracene-derived KITPHOS units, from 38.0 to 58.4 (entries 1-3), while the corresponding values for their unsubstituted counterparts are all significantly smaller and increase gradually from 30.0 to 33.6 (entries 4-6). The difference in the calculated G parameters of 8.0 between **8a** (38.0) and **8d** (30.0) is much smaller than the corresponding difference of 20.7 for PPh_3 and PPh_2(*o*-biphenyl) (entries 7 and 10, respectively), which further supports the disparate effect on steric properties of introducing a proximal phenyl ring onto an aryl-like KITPHOS monophosphine compared with its aryl counterpart, as noted above for the trend in $\%V_{bur}$. Although further studies and data will be required to lend validity to this interpretation, the introduction of a single proximal phenyl ring into triphenylphosphine appears to have a more marked and profound influence on steric congestion than for KITPHOS monophosphines.

Table 2. Comparison of G Parameters and Associated Cone Angles for KITPHOS Monophosphines and Selected Triarylphosphines[a]

entry	phosphine	G param[a]	cone angle θ/deg[b]
1	Ph-MONOKITPHOS (**8a**)	38.0	152.2
2	Ph-BISKITPHOS (**8b**)	47.6	174.5
3	Ph-TRISKITPHOS (**8c**)	58.4	199.4
4	H-MONOKITPHOS (**8d**)	30.0	132.8
5	H-BISKITPHOS	31.8	137.2
6	H-TRISKITPHOS	33.6	141.7
7	PPh_3	27.8	127.0
8	$PMes_3$	59.3	201.4
9	Bowl-shaped Phos[16]	43.6	165.2
10	PPh_2(o-biphenyl)	48.5	176.5

[a]Calculated using Solid-G.[48] [b]Equivalent cone angle calculated from the non-linear relationship $\Omega = 100[1 - \cos\left(\frac{\theta}{2}\right)]$ where $G = 100\frac{\Omega}{4\pi}$

Gold-Catalyzed C-O and C-N Bond-Forming Cycloisomerizations. Having previously demonstrated that gold(I) complexes of electron-rich KITPHOS monophosphines form highly efficient catalysts for the cycloisomerization of propargyl amides[24] and reasoning that their electron-deficient sterically-tunable triaryl-like counterparts **8a-d** would both enhance Lewis acidity and enable substrate accessibly to be modulated in a systematic manner, we chose this transformation to conduct an initial comparison and evaluation of the performance of **9a-d** against PPh_3AuCl; full details are listed in Table 3.

Table 3. Comparison of the 5-*Exo*-dig Cycloisomerization of Propargyl-Amides 10a-e Catalyzed by Gold Complexes of KITPHOS Monophosphines 8a-d and PPh_3[a]

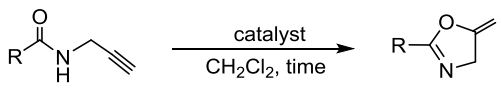

10a-e **11a-e**

entry	substrate	precatalyst	Time (h)	Yield (%)[b]
1[c]		**9a**	0.5	76
2	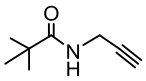	**9b**	0.5	92
3		**9c**	0.5	1
4	**10a**	**9d**	0.5	51
5		PPh_3AuCl	0.5	50
6[c]		**9a**	0.5	71
7	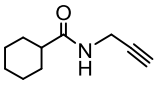	**9b**	0.5	99
8		**9c**	0.5	4
9	**10b**	**9d**	0.5	62
10		PPh_3AuCl	0.5	41
11[c]		**9a**	1.5	88
12	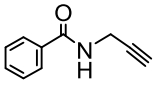	**9b**	1.5	98
13		**9c**	1.5	4
14	**10c**	**9d**	1.5	69
15		PPh_3AuCl	1.5	54
16[c]		**9a**	4	84
17	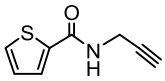	**9b**	4	43
18		**9c**	4	24
19	**10d**	**9d**	4	44
20		PPh_3AuCl	4	42
21[c]		**9a**	1.5	80
22	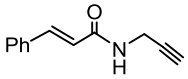	**9b**	1.5	77
23		**9c**	1.5	7
24	**10e**	**9d**	1.5	39
25		PPh_3AuCl	1.5	34

[a]Reaction conditions: 2 mol% **9a-d** or PPh_3AuCl, 2 mol% AgOTf, 0.5 mmol propargyl amide, CH_2Cl_2, time, room temperature. [b]Isolated yields. Average of three runs. [c]Data obtained from the literature.[24]

In a typical reaction, catalyst was generated in situ immediately prior to addition of substrate by treating a dichloromethane solution of the corresponding gold(I) chloride precatalyst with silver triflate for 30 min. Under these conditions catalysts formed from **9a** and **9b** both gave excellent conversions for each of the substrates tested (**10a-e**) and both consistently outperformed their triphenylphosphine counterpart, in some cases by quite some margin. For comparison, catalyst generated from **9c** gave poor conversions under the same conditions and in the same time, which may be due to restricted access of the substrate to the gold center, which is effectively surrounded by or embedded deep in the triaryl-like cavity. As the proximal aryl ring of biaryl monophosphines

has been proposed to stabilize catalytic intermediates with respect to deactivation through formation of a weak arene-gold interaction,[49] comparative catalyst testing was extended to **9d** in order to investigate the influence on efficiency of removing the proximal biaryl-like aryl ring from **9a**. The data in Table 3 reveals that the conversions obtained with **9d** are consistently lower than those obtained with its biaryl-like counterpart and more closely correlate with those obtained with triphenylphosphine; further evidence that a proximal phenyl ring can exert a positive effect on catalyst performance. In this regard, Hammond and Xu have recently highlighted the importance of ortho substitution and electron density matching within the ligand.[38a] The former was suggested to prevent deactivation of the catalyst by forming weakly stabilizing Au---C interactions while the latter facilitates regeneration of the cationic gold catalyst by favoring turnover-limiting protodeauration of the intermediate gold σ-complex.[50b] Since a slight excess of silver triflate is typically used to ensure quantitative activation of the precatalyst and Lewis acid silver salts have been reported to activate alkynes towards cycloisomerization,[51] a series of parallel catalytic control experiments were conducted under the same conditions with 2 mol% AgOTf in the absence of precatalyst. Although these experiments conclusively show that AgOTf is not an active cycloisomerization catalyst for propargyl amides, they do not exclude a more subtle role for adventitious silver such as interception of gold(I) intermediates, as recently reported by Gagné and co-workers[52a] or even false negative results due to formation of a less active chloride bridged digold complex.[52b,c]

The cycloisomerization-derived methylene oxazolines **11a-e** were considered ideal candidates for use as the olefinic partner in the carbonyl-ene reaction; the resulting products would be synthetically versatile *β*-hydroxy, β-ester-substituted oxazolines **12a-d** (Table 4). With the aim of developing a single–pot tandem reaction sequence based on cycloisomerization of propargyl amides **10a-e** followed by a Lewis acid-catalyzed asymmetric carbonyl-ene reaction with the resulting methylene oxazoline enophile, the reaction of a purified sample of **11a-e** towards ethyl trifluoropyruvate was examined using previously optimized conditions and catalysts for the corresponding reaction between methylene cyclopentane and ethyl trifluoropyruvate as a lead.[53] Following a previously optimized protocol, 5 mol% (*S*)-$PdCl_2$(BINAP)/$AgSbF_6$ catalyzed the carbonyl-ene reaction between methylene cyclopentane and ethyl trifluoropyruvate with remarkable efficiency and gave the expected α-hydroxy ester in excellent yield and 98% ee after only 30 min at room temperature. However, disappointingly, under the same conditions the corresponding reaction between **11a-d** and ethyl trifluoropyruvate gave the desired product in near quantitative yield but as a racemic mixture. As copper(II) complexes of bis(oxazolines) are among the most efficient catalysts for the carbonyl-ene reaction an optimized literature protocol was also applied to the reaction between **11a-d** and methylene cyclopentane.[54] Again, while quantitative yields were also obtained in short reaction times, in each case the product was isolated as a racemic mixture. Interestingly, quantitative yields were also obtained in control reactions conducted in the absence of catalyst, which strongly suggests that the racemic product results from a competing uncatalyzed process. Even though we have not been able to develop an asymmetric version of the methylene oxazoline-based carbonyl-ene reaction, the rapid uncatalyzed nature of this transformation enabled a tandem single-pot protocol for the synthesis of highly functionalized 2-substituted oxazolines to be developed with each step proceeding in excellent conversion to afford **12a-d** in high yields.

Table 4. Carbonyl-ene Reaction between Oxazolines 11a-d and Ethyl Trifluoropyruvate[a]

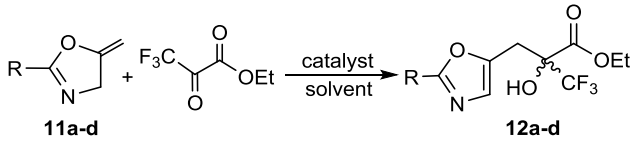

11a-d **12a-d**

entry	R	compound	Yield (%)
1	tert-Bu	**12a**	94
2	C_6H_{11}	**12b**	95
3	C_6H_5	**12c**	91
4	2-thienyl	**12d**	94

[a] 5 mol% [$PdCl_2${(*S*)-BINAP}]/5 mol% $AgSBF_6$, CH_2Cl_2, 30 min, room temperature

Encouraged by the efficiency of **8a-b** as ligands for the gold-catalyzed cycloisomerization of propargyl amides, comparative catalyst testing was extended to include the regioselective C-O bond forming cycloisomerization of 2-alkynylbenzyl alcohols to generate isochromenes with the aim of investigating whether steric bulk influences *endo/exo*-dig selectivity. These heterocycles are important targets as they are found in a host of bioactive compounds with a range of therapeutic properties including activity against various human cancer cells lines as well as antioxidant and antifungal properties.[28] While a gold(I) complex of trimesitylphosphine catalyzes the selective 6-*endo*-dig cycloisomerization of 2-alkynylbenzyl alcohols to afford the corresponding isochromenes, a high catalyst loading (5.0 mol%) and/or long reaction time was required to achieve acceptable yields across only a limited range of substrates.[55] Similarly, iridium(III) hydride complexes also catalyze the selective 6-*endo*-dig cyclization of these substrates but a catalyst loading of 4 mol% and reaction temperatures between 60 ºC and 85 °C was required to obtain high conversions.[56] Our preliminary evaluation focused on the selective 6-*endo*-dig cyclization of 2-hex-1-ynylbenzyl alcohol **13a** to afford isochromene **14a** using 0.5 mol% of gold precatalyst activated with AgOTf in dichloromethane at room temperature (Table 5). Under these conditions, **9a** gave the desired isochromene in 98% yield whereas the sterically more congested **9b** and **9c** gave markedly lower conversions of 64% and 19%, respectively (entries 1–3). Parallel catalyst testing with **9d**, which lacks a proximal phenyl ring, gave the 6-*endo*-dig product in 37% yield under the same conditions (entry 4), which is comparable to the yield of 27% obtained with PPh_3AuCl/AgOTf (entry 5). Encouraged by the high conversions obtained with **9a** after short reaction times and under mild conditions, catalyst testing was extended to include the cyclization of a series of 2-alkynylbenzyl alcohols, 2-(2-(phenylethynyl)phenyl)ethan-1-ol and 2-(phenylethynyl)benzoic acid, details of which are summarized in Tables 4–5 and Equation 2. Excellent conversions and

complete 6-*endo*-dig regioselectivity were obtained for the cycloisomerization of **13b** and **13c** with 0.5 mol% **9a**/AgOTf which gave the corresponding isochromenes as the sole product after only 1 h at room temperature (entries 7 and 10).

Table 5. Gold-Catalyzed Cycloisomerization of 2-Alkynylbenzyl Alcohols[a]

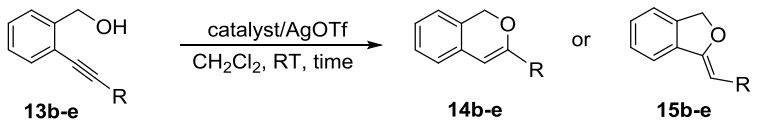

entry	substrate	catalyst	mol%	Time (h)	% conversion[b]	**14:15**
1		**9a**	0.5	1	98	1:0
2	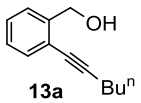 **13a**	**9b**	0.5	1	64	1:0
3		**9c**	0.5	1	19	1:0
4		**9d**	0.5	1	37	1:0
5		Ph_3PAuCl	0.5	1	27	1:0
6		AgOTf	2.0	1	13	1:0
7	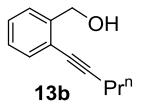 **13b**	**9a**	0.5	1	98	1:0
8		AgOTf	2.0	1	7	1:0
9		$[(Mes_3PAu)_2Cl][BF_4]$[c]	2.5	24	31	1:0
10	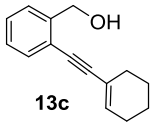 **13c**	**9a**	0.5	1	90	1:0
11		AgOTf	2.0	1	8	1:0
12	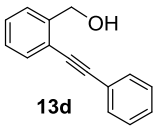 **13d**	**9a**	2.0	16	100	1:0
13		AgOTf	2.0	16	64	1:0
14		$[(Mes_3PAu)_2Cl][BF_4]$[c]	5.0	24	75	1:0
15	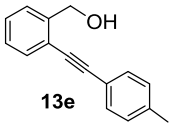 **13e**	**9a**	0.5	1	100	1:0.4
16		AgOTf	2.0	16	46	1:0.92

[a]Reaction conditions: 0.5–2.0 mol% **9a**/0.5–2.0 mol% AgOTf or 0.5–2.0 mol% AgOTf, 0.4 mmol 2-alkynylbenzyl alcohol, CH_2Cl_2, time, room temperature. [b]Conversions determined by ^{1}H NMR spectroscopy using 1,3-dinitrobenzene as internal standard. Average of three runs. [c]2.5–5.0 mol% precatalyst, data obtained from the literature.[55]

The conversion of 98% obtained for **13b** is a quite remarkable in comparison to the 31% yield reported for the same transformation using 2.5 mol% $[(Mes_3PAu)_2Cl][BF_4]$ and a reaction time of 24 h (entry 9).[55] The cyclization of **13d** was markedly more challenging and required 2 mol% **9a**/AgOTf and a reaction time 16 h to reach complete conversion to the 6-e*ndo*-dig regioisomer (entry 12). Gratifyingly, regardless of the extended reaction times, **9a** either competed with or outperformed previously reported systems for this transformation including $[(Mes_3PAu)_2Cl][BF_4]$, which required a catalyst loading of 5 mol% to reach 75% conversion after 24 h (entry 14) and $[IrH(2\text{-acetylphenyl})(acetone)(PPh_3)_2]SbF_6$ which gave isochromene **13d** in 70% yield after 2 h at 85 ºC in the presence of 3 mol% catalyst. In contrast, the corresponding *p*-tolyl-substituted 2-alkynylbenzyl alcohol **13e** only required 0.5 mol% **9a**/AgOTf and a reaction time of 1 h to reach 100% conversion and even though the 6-*endo*-dig regioisomer was the major product, formation of 5-*exo*-dig regioisomer was rather unexpected considering the minor structural/electronic difference between **13d** and **13e** (entry 15). At this stage we cannot offer a conclusive explanation for this change in selectivity but note that a mixture of regioisomers has previously been obtained from the gold-catalyzed cycloisomerization of 2-nitro-1-(2-(arylethynyl)phenyl)ethan-1-ols, generated *in situ* via a copper-catalyzed asymmetric Henry reaction between a *o*-alkynylbenzaldehyde and nitromethane; in general, electron-donating groups on the alkynyl fragment favored the 6-*endo*-dig pathway while those with electron-withdrawing groups favored 5-*exo*-dig cyclization.[57] There have been several reports of the synthesis of 1*H*-isochromenes based on the domino addition/cycloisomerization of an alkynylbenzaldehyde in the presence of a protic nucleophile and a carbophilic silver,[51b,c,e,58a] gold[58b] or indium[58c] Lewis acid catalyst, however, in each case

the loading was markedly higher than the 0.5 mol% required for the **9a**/AgOTf catalyzed cyclizations described here. A series of parallel control experiments in the presence of 2 mol% AgOTf gave low conversion under the same conditions, even after extend reaction times, which provide convincing evidence for catalysis by a gold(I) species (entries 6, 8, 11, 13 and 15).

The competitive performance of **9a** prompted us to explore its efficacy as a catalyst for the cyclization of 2-(2-(phenylethynyl)phenyl)ethan-1-ol **16**, a substrate that has previously been reported to be unreactive towards cyclization by iridium-hydride and gold-phosphine based systems (Equation 2).[55,56] Reassuringly, 2 mol% **9a**/AgOTf catalyzed this transformation with remarkable efficacy and reached 100% conversion to afford a 89:11 mixture of 1-benzylideneisochromane **17** and 4-phenyl-1,2-dihydrobenzo[d]oxepine **18** after 16 h at room temperature; the two isomers were distinguished, identified and their structures confirmed by the use of an INADEQUATE spectrum. During the preparation of this manuscript, Naoe *et al*. reported the first example of this cyclization and obtained an 87:13 mixture of products in favor of the 6-*exo*-dig regioisomer by using 5 mol% IPrAuCl/AgOTf at 50 ºC.[59] While the observed selectivity is entirely in keeping with previous examples of gold-catalyzed cyclizations involving alkynes,[60] there have been reports of 7-*endo*-dig cyclization involving terminal and arylated alkynes.[61] For example, gold(I) complexes of electron deficient hollow-shaped triethynylphosphines are the ligands of choice for 6-*exo*- and 7-*endo*-dig cyclizations involving tethered alkynes; their efficiency of these systems compare with conventional phosphines was proposed to be associated with the cavity of the ligand which forces the nucleophile in close proximity to the gold-activated alkyne.[61h,i]

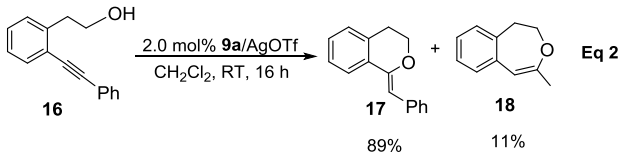

While the cyclization of 2-alkynylbenzoic acids provides access to 5- and 6-membered lactones and can be catalyzed by strong acids, palladium, gold or silver compounds, products are often obtained as a mixture of regioisomers.[62] For example, AuCl-catalyzed lactonization of **19** occurs with a marked preference for 5-*exo*-dig cyclization to afford a 91:9 mixture of the exo and endo regioisomers, **20** and **21**, respectively,[62b] and the corresponding palladium-catalyzed transformation also occurs with moderate 5-*exo*-dig selectivity to afford a 56:23 mixture of regioisomers (Table 6 entries 1-2).[62d] Interestingly, in a comparative study 0.5 mol% **9a**/AgOTf catalyzed the cyclization of **19** with remarkable efficiency but gave a complete switch in selectivity to afford the 6-*endo*-dig regioisomer as the exclusive product, in near quantitative yield after only 15 min at room temperature (Table 6 entry 3). Such a dramatic change in selectivity and improvement in efficiency is intriguing and further studies are clearly required to explore and develop an understanding of the factors that control the regioselectivity of this transformation.

Finally, the high yields obtained for the cyclization of 2-alkynylbenzoic acids, the switch in regioselectivity and the close similarity between the bioactivity of isocoumarins and their nitrogen based 1*H*-isochromene-1-imine counterparts prompted us to apply the same system to the intramolecular cycloisomerization of 2–(phenylethynyl)benzamides **22a-c** (Table 7). Under the same conditions, 2 mol% **9a**/AgOTf catalyzed the 6-*endo*-dig *O*-cyclization of **22a-c** to give good yields of the corresponding 1*H*-isochromene-1-imine in reasonably short reaction times and with no evidence for competing 5-*exo*-dig or *N*-6-*endo*-dig cyclization. As far as we are aware there have been no reports of the gold(I)-catalyzed cycloisomerization of 2–(phenylethynyl)benzamides for a direct comparison, however, **9a**/AgOTf competes with AgOTf in dichloroethane and outperforms $AgSbF_6$ in toluene which requires a higher reaction temperature, longer reaction time and 25 mol% catalyst to achieve acceptable yields of the 6-*endo*-dig cyclization product.[63a,b] In a more recent development, a copper-mediated coupling-cyclization sequence between a 2-iodobenzamide and a terminal alkyne occurred via the 6-*endo*-dig pathway to provide a complimentary pathway to isoquinolin-1(2*H*)-ones; however, further studies will be required to assess the relative merits of this system against our KITPHOS-based gold catalysts.[64] As **9a**/AgOTf forms an efficient and selective catalyst for the 6-*endo*-dig cyclization of 2–(phenylethynyl)benzamides, it will be interesting to apply this combination to the cycloisomerization of 2-(1-alkynyl)phenylacetamides as this reaction has recently been catalyzed by $PPh_3AuCl/AgSbF_6$ with complete 7-*endo*-dig selectivity, however, 10 mol% catalyst and a reaction temperature of 120 ºC was required to achieve practical yields.[61d,e,g] On the basis that silver salts have been reported to catalyze this cyclization a series of control experiments were conducted under identical conditions with 5 mol% AgOTf. Even though slightly higher yields were obtained with AgOTf than **9a**/AgOTf for each substrate tested we are confident that the yields obtained with **9a** reflect the activity of an electrophilic gold cation as there is a reassuringly close correlation between the performance of catalyst generated in situ and its isolated cation [AuL]OTf.[24]

Table 6. Comparison of the Cycloisomerization of 2-Alkynylbenzoic Acid Catalyzed by 9a, AuCl and $PdCl(MeCN)_2$[a]

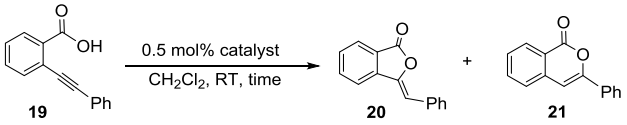

	catalyst	mol%	time	conversion[b]	20:21
1	$AuCl/AgNTf_2$	5.0	2 h	82	1:0.1
2	$PdCl_2(MeCN)_2$	10.0	24 h	89	1:0.4
3	**9a**/AgOTf	0.5	15 min	100	0:1

[a]Reaction conditions: 0.5 mol% **9a**/0.5 mol% AgOTf, 0.4 mmol 2-alkynylbenzoic acid, CH_2Cl_2, time, room temperature. [b]Conversions determined by ^1H NMR spectroscopy using 1,3-dinitrobenzene as internal standard. Average of three runs.

Table 7. Comparison of the Gold-Catalyzed 6-*Endo*-Dig Cycloisomerization of 2-(Phenylethynyl)benzamides 22a-c against AgOTf[a]

entry	Substrate	catalyst	mol%	product	Time (h)	Yield (%)[b]
1	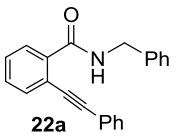 **22a**	**9a**/AgOTf	2	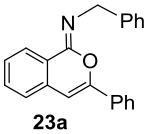 **23a**	3	71
2		AgOTf	2		3	90
3	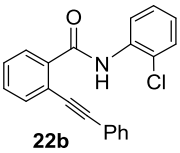 **22b**	**9a**/AgOTf	2	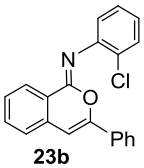 **23b**	2	57
4		AgOTf	2		2	66
5	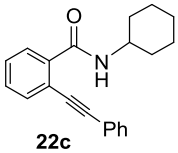 **22c**	**9a**/AgOTf	2	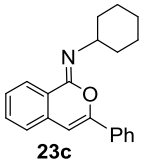 **23c**	2	66
6		AgOTf	2		2	53

[a]Reaction conditions: 2.0 mol% **9a**/2.0 mol% AgOTf or 2.0 mol% AgOTf, 0.4 mmol 2-(phenylethynyl)benzamide, $CHCl_3$, time, 60 ºC. [b]Yields determined by ^1H NMR spectroscopy using dinitrobenzene as internal standard. Average of three runs.

CONCLUSIONS

Gold(I) complexes of electron-deficient triaryl-like MONOKITPHOS and BISKITPHOS monophosphines containing one and two 12-phenyl-9,10-dihydro-9,10-etheno-anthracene units, respectively, are markedly more efficient catalysts than their triphenylphosphine counterpart for a range of carbon-heteroatom bond-forming cyclizations whereas the corresponding TRISKITPHOS–based catalyst gave low conversions. Moreover, we present the first examples of gold(I)-catalyzed 6-*endo*-dig cycloisomerizations involving 2-(phenylethynyl) benzamides and gratifyingly gold(I)/MONOKITPHOS either rivals or outperforms all existing silver and palladium-based systems. Interestingly, TRISKITPHOS monophosphine bears a close architectural similarity to the bowl-shaped class of phosphine in that the bulkiness occurs at the periphery with the proximal aryl-like phenyl rings orientated towards the rim of the bowl. In this regard, even though TRISKITPHOS is not an effective ligand for gold-catalyzed cycloisomerizations, the unique catalytic environment presented by the array of anthracene-derived biaryl-like units and the steric bulk of this phosphine could stabilize active low-coordinate species while allowing substrate access. The high level of internal steric congestion in Ph-TRISKITPHOS, its oxide and the corresponding gold(I) chloride is responsible for hindered rotation about the P-C bond which lowers the molecular symmetry such that the two C_6H_4 rings in each of the 12-phenyl-9,10-dihydro-9,10-etheno-anthracene units become inequivalent; a lower energy process involving restricted rotation of the biaryl-like phenyl ring has also identified in a detailed and thorough solution NMR study. Although this investigation has been restricted to a relatively narrow range of cyclizations the high yields obtained across a diverse and challenging range of substrates at low catalyst loadings and under mild conditions is extremely encouraging which suggests that this system may be an ideal candidate for use in reaction development.

ASSOCIATED CONTENT

Supporting Information

The Supporting Information is available free of charge on the ACS Publications website. Full details of experimental procedures, characterization data for all new compounds, figures showing the variable temperature ^1H NMR spectra and selected COSY, EXSY, NOESY, ROESY, HSQC and HMBC 2D-spectra for compounds **7c**, **8c** and **9c**, details of catalyst testing (PDF) and X-ray crystallographic data for compounds **7c** and **9a-d** (CIF). Crystallographic data can also be obtained free of charge from the Cambridge Crystallographic Data Centre (CCDC 1454006, 1454008, 1454009, 1454010 and 1455028) via www.ccdc.cam.ac.uk/data_request/cif.

AUTHOR INFORMATION

Corresponding Author

* E-mail: simon.doherty@ncl.ac.uk (S.D.)

Notes

The authors declare no competing financial interest.

ACKNOWLEDGMENT

We gratefully acknowledge Newcastle University for funding (N.A.B.W. and D.O.P) and Johnson Matthey for generous loans of palladium salts. We acknowledge the use of the EPSRC UK

National Service for Computational Chemistry Software (NSCCS) at Imperial College London in carrying out this work. Many thanks to Elwood, Jake and Ella for their loyal and unwavering support. This paper is dedicated to the memory of Professor Malcolm H. Chisholm (FRS).

EXPERIMENTAL SECTION

General Procedure for the Gold-Catalyzed Cycloisomerization of Propargyl Amides. A flame-dried Schlenk flask charged with precatalyst LAuCl (0.01 mmol), AgOTf (0.0026 g, 0.01 mmol) and dichloromethane (2 mL) was stirred for 30 min after which propargyl amide (0.5 mmol) was added and the reaction mixture stirred at room temperature for the allocated time. The reaction mixture was diluted with diethyl ether, 1,3-dinitrobenzene (0.084 g, 0.5 mmol) added as an internal standard and the resulting mixture was passed through a short silica plug, flushing with ethyl acetate. The solvent was removed under reduced pressure and the residue analyzed by ^{1}H NMR spectroscopy to determine the conversion before being purified by column chromatography, eluting with hexane/ethyl acetate; all know products were characterized by NMR spectroscopy and mass spectrometry.

General Procedure for the Carbonyl-Ene Reaction between Methylene Oxazoline and Ethyl Trifluoropyruvate. A flame-dried Schlenk flask was charged with $PdCl_2$(BINAP) (0.020 g, 25 μmol), $AgSbF_6$ (0.0137 g, 50 μmol)* and dichloromethane (2 mL) and the mixture stirred for 0.5 h to generate the active catalyst. After this time methylene oxazoline (0.5 mmol) and ethyl trifluoropyruvate (0.75 mmol) were added and the reaction stirred at room temperature for the specified time. Decane (0.097 mL, 0.5 mmol) was added as internal standard and the reaction passed through a short silica plug with ethyl acetate. The solvent was removed under reduced pressure and the residue analyzed by gas chromatography to determine the conversion and enantioselectivity. Known products were characterized by NMR spectroscopy and mass spectrometry. (*or $Cu(OTf)_2$ (0.018 g, 50 μmol) and BOX (2,2′-isopropylene bis[(4*S*)-4-*tert*-butyl-2-oxazoline]) (0.015 g, 50 μmol) was used to generate the catalyst).

General Procedure for Gold-Catalyzed Cycloisomerization 2–Alkynylbenzyl Alcohols 2-(2-Phenylethynyl)benzoic Acid and 2-(Phenylethynyl)benzamides. A flame-dried Schlenk flask charged with precatalyst LAuCl (0.5-5.0 mol%, 0.0025-0.025 mmol), AgOTf (0.5-5.0 mol%, 0.0025-0.025 mmol) and dichloromethane (2 mL) was stirred for 30 min, after which substrate (0.5 mmol) was added and the reaction mixture stirred at an appropriate temperature for the allocated time.* The reaction mixture was diluted with diethyl ether, 1,3-dinitrobenzene (0.084 g, 0.5 mmol) added as internal standard and the resulting mixture passed through a short silica plug and flushed with ethyl acetate. The solvent was removed under reduced pressure and the residue analyzed by ^{1}H NMR spectroscopy to determine the conversion before being purified by column chromatography with hexane/ethyl acetate as eluant; known products were characterized by NMR spectroscopy and mass spectrometry and unknown products by NMR spectroscopy, mass spectrometry, high resolution mass spectrometry (HRMS) and elemental analysis. (* For reactions using AgOTf as catalyst, the solution was also stirred for 30 min before substrate was added).

REFERENCES

(1) For a selection of highly informative reviews see: (a) Fleckenstein, C. A.; Plenio, H. *Chem. Rev*. **2010**, *39*, 694–711. (b) Fu, G. C. *Acc. Chem. Res*. **2008**, *41*, 1555–1564. (c) Surry, D. S.; Buchwald, S. L. *Angew. Chem. Int. Ed*. **2008**, *47*, 6338–6361. (d) Martin, R.; Buchwald, S. L. *Acc. Chem. Res*. **2008**, *41*, 1461–1473. (e) Surry, D. S.; Buchwald, S. L. *Chem. Sci*. **2011**, *2*, 27–50. (f) Maiti, F.; Fors, B. P.; Henderson, J. L.; Nakamura, Y.; Buchwald, S. L. *Chem. Sci*. **2011**, *2*, 57–68. (g) Buchwald, S. L.; Mauger, C.; Mignani, G.; Scholz, U. *Adv. Synth. Catal*. **2006**, *348*, 23–39. (h) Zapf, A.; Beller, M. *Chem. Commun*. **2005**, 431-440. (i) Magano, J.; Dunetz, J. R. *Chem. Rev*. **2011**, *111*, 2177–2250. (j) Torborg, C.; Beller, M. *Adv. Synth. Catal*. **2009**, *351*, 3027–3043.

(2) (a) Wolfe, J. P.; Buchwald, S. L. *Angew. Chem. Int. Ed*. **1999**, *38*, 2413–2416. (b) Wolfe, J. P.; Tomori, H.; Sadighi, J. P.; Yin, J. J.; Buchwald, S. L. *J. Org. Chem*. **2000**, *65*, 1158–1174.

(3) (a) Christmann, U.; Villar, R. *Angew. Chem. Int. Ed*. **2005**, *44*, 366–374. (b) Roy, A. H.; Hartwig, J. F. *Organometallics* **2004**, *23*, 194–202. (c) Barrios-Landeros, F.; Hartwig, J. F. *J. Am. Chem. Soc*. **2005**, *127*, 6944–6945. (d) Hills, I. D.; Netherton, M. R.; Fu, G. C. *Angew. Chem. Int. Ed*. **2003**, *42*, 5749–5752.

(4) (a) Barder, T. E.; Biscoe, M. R.; Buchwald, S. L. *Organometallics* **2007**, *26*, 2183–2192. (b) Bader, T. E.; Buchwald, S. L. *J. Am. Chem. Soc*. **2007**, *129*, 12003–12010. (c) Biscoe, M. R.; Bader, T. E.; Buchwald, S. L. *Angew. Chem. Int. Ed*. **2007**, *46*, 7232–7235. (d) Christmann, U.; Panatazis, D. A.; Benet-Buchholz, J.; McGrady, J. E.; Maseras, F.; Vilar, R. *J. Am. Chem. Soc*. **2006**, *128*, 6376–6390.

(5) (a) Biscoe, M. R.; Fors, B. P.; Buchwald, S. L. *J. Am. Chem. Soc*. **2008**, *130*, 6686–6687. (b) Kinzel, T.; Zhang, Y.; Buchwald, S. L. *J. Am. Chem. Soc*. **2010**, *132*, 14073–14075. (c) Bruno, N. C. Buchwald, S. L. *Org. Lett*. **2013**, *15*, 2876–2879. For insightful reviews and edge articles see: (d) Bruno, N. C.; Tudge, M. T.; Buchwald, S. L. *Chem. Sci*. **2013**, *4*, 916–920. (e) Bruneau, A. Roche, M.; Alami, M.; Messaoudi, S. *ACS Catal*. **2015**, *5*, 1386–1396.

(6) (a) Zapf, A.; Jackstell, R.; Rataboul, F.; Riermeier, T.; Monsees, A.; Fuhrmann, C.; Shaikh, N.; Dingerdissen, U.; Beller, M. *Chem. Commun*. **2004**, 38. (b) Harkal, S.; Rataboul, F.; Zapf, A.; Fuhrmann, C.; Reirmeier, T.; Monsees, A.; Beller, M. *Adv. Synth. Catal*. **2005**, *346*, 1742.

(7) (a) So, C. M.; Lau, C. P.; Kwong, F. Y. *Angew. Chem. Int. Ed*. **2008**, *47*, 8059–8063. (b) So, C. M.; Yeung, C. C.; Lau, C. P.; Kwong, F. Y. *J. Org. Chem*. **2008**, *73*, 7803–7806. (c) So, C. M.; Lau, C. P.; Chan, A. S.; C.; Kwong, F. Y. *J. Org. Chem*. **2008**, *73*, 7731–7734. (d) So, C. M.; Zhou, Z.; Lau, C. P.; Kwong, F. Y. *Angew. Chem. Int. Ed.* **2008**, *47*, 6402–6406. (e) So, C. M.; Lau, C. P.; Kwong, F. Y. *Org. Lett*. **2007**, *9*, 2795–2798. (f) So, C. M.; Lee, H. W.; Lau, C. P.; Kwong, F. Y. *Org. Lett*. **2009**, *11*, 317–320. (g) Yeung, P. Y.; So, C. M.; Lau, C. P.; Kwong, F. Y. *Angew. Chem. Int. Ed*. **2010**, *49*, 8918–8922. (h) Yeung, P. Y.; Chung, K. H.; Kwong, F. Y. *Org. Lett*. **2011**, *13*, 2912–2915.

(8) (a) Singer, R. A.; Caron, S.; Dermott, R. E.; Arpin, P.; Do, N. M. *Synthesis* **2002**, 1727–1731. (b) Singer, R. A.; Dore, M.; Sieser, J. E.; Berliner, M. A. *Tetrahedron Lett*. **2006**, *47*, 3727–3731.

(9) Withbroe, G. J.; Singer, R. A.; Sieser, J. E. *Org. Process Res. Dev*. **2008**, *12*, 480–489.

(10) (a) Lundgren, R. J.; Peters, B. D.; Alsabeh, P. G.; Stradiotto, M. *Angew. Chem. Int. Ed*. **2010**, *49*, 4071–4074. (b) Lundgren, R. J.; Stradiotto, M. *Angew. Chem. Int. Ed*. **2010**, *49*, 8686–8690. (c) Hesp, K. D.; Lundgren, R. J.; Stradiotto, M. *J. Am. Chem. Soc*. **2011**, *133*, 5194–5197. (d) Lundgren, R. J.; Sappong-Kumankumah, A.; Stradiotto, M. *Chem. Eur. J*. **2010**, *16*, 1983–1991. (e) Hesp, K. D.; Stradiotto, M. *J. Am. Chem. Soc*. **2010**, *132*, 18026–18029.

(11) (a) Tang, W.; Capacci, A. G.; Wei, X.; Li, W.; White, A.; Patel, N. D.; Savoie, J.; Gao, J. J.; Rodriguez, S.; Qu, B.; Haddad, N.; Lu, B. Z.; Krishnamurthy, D.; Lee, N. K.; Senanayake, C. H. *Angew Chem. Int. Ed*. **2010**, *49*, 5879–5873; *Angew. Chem*. **2010**, *122*, 6016. (b) Tang, W.; Keshipeddy, S.; Zhang, Y.; Wei, Z.; Sacoie, J.; Patel, N. D.; Yee, N. K.; Senanayake, C. H. *Org. Lett*. **2011**, *13*, 1366–1369. (c) Rodriguez, S.; Qu, B.; Haddad, N.; Re`eves, D.; Tang, W.; Krishnamurthy, D.; Senanayake, C. H. *Adv. Synth. Catal*. **2011**, *353*, 533–537.

(12) Kwong, F. Y.; Chan, K. S.; Yeung, C. H.; Chan, A. S. C. *Chem. Commun.* **2004**, 2336–2337.

(13) (a) Malacea, R.; Saffon, N.; Gómez, M.; Bourissou, D. *Chem. Commun*. **2011,** *47*, 8163–8165. (b) Malacea, R.; Chahdoura, F.; Devillard, M.; Saffon, N.; Gómez, M.; Bourissou, D. *Adv. Synth. Catal*. **2013,** *355*, 2274–2284.

(14) So, C. M.; Chow, W. K.; Choy, P. Y.; Lau, C. P.; Kwong, F. Y. *Chem. Eur. J*. **2010**, *16*, 7996–8001.

(15) Snelders, D. J. M.; Kreiter, R.; Firet, J. J.; van Koten, G.; Klein Gebbink, R. J. M. *Adv. Synth. Catal*. **2008**, *350*, 262–266.

(16) (a) Fujihara, T.; Semba, K.; Terao, J.; Tsuji, Y. *Angew. Chem. Int. Ed*. **2010**, *49*, 1472–1476. (b) Niyomura, O.; Iwasawa, T.; Sawada, N.; Tokunaga, M.; Obora, Y.; Tsuji, Y. *Organometallics* **2005**, *24*, 3468–3475.

(17) René, O.; Fagnou, K. *Adv. Synth. Catal*. **2010**, 3*52*, 2116–2120.

(18) Hesp, K. D.; Lundgren, R. J.; Stradiotto, M. *J. Am. Chem. Soc*. **2011**, *133*, 5194–5197.

(19) Chow, W. K.; Yuen, O. Y.; So, C. M.; Wong, W. T.; Kwong, F. Y. *J. Org. Chem*. **2012**, *77*, 3543–3548.

(20) Tschan, M. J.-L.; García-Suárez, E. J.; Freixa, Z.; Launay, H.; Hagen, H.; Benet-Buchholz, J.; van Leeuwen, P. W. N. M. *J. Am. Chem. Soc*. **2010**, *132*, 6463–6473.

(21) (a). Doherty, S.; Smyth, C. H.; Knight, J. G.; Hashmi, A. S. K. *Nature Protocols* **2012**, *7*, 1870–1883 (b) Doherty, S.; Smyth, C. H. *Nature Protocols* **2012**, *7*, 1884–1896.

(22) (a) Doherty, S.; Knight, J. G.; Smyth, C. H.; Jorgensen, G. A. *Adv. Synth. Catal*. **2008**, *350*, 1801–1806. (b) Doherty, S.; Knight, J. G.; McGrady, J. P.; Ferguson, A. M.; Ward, N. A. B.; Harrington R. W.; Clegg, W. *Adv. Synth. Catal*. **2010**, *352*, 201–211. (c) Doherty, S.; Knight, J. G.; Ward, N. A. B.; Bittner, D. M.; Wills, C.; McFarlane, W.; Clegg, W.; Harrington, R. W. O*rganometallics* **2013**, *32*, 1773–1788. (d) Doherty, S.; Knight, J. G.; Ward, N. A. B.; Perry, D. O.; Bittner, D. M.; Probert, M. R.; Westcott, S. A. *Organometallics* **2014**, *33*, 5209–5219.

(23) (a) Hashmi, A. S. K.; Loos, A. Littmann, A.; Braun, I.; Knight, J. G.; Doherty, S.; Rominger, F. *Adv. Synth. Catal*. **2009**, *351*, 576–582. (b) Hashmi, A. S. K.; Loos, A.; Doherty, S.; Knight. J. G.; Robson, K. J.; Rominger, F. *Adv. Synth. Catal*. **2011**, *353*, 749–759.

(24) Doherty, S.; Knight, J. G.; Smyth, C. H.; Ward, N. A. B.; Robson, K. J.; Tweedly, S.; Harrington, R. W.; Clegg, W. *Organometallics*, **2010**, *29*, 4139–4157.

(25) Doherty, S.; Knight, J. G.; Addyman, C. R.; Smyth, C. H.; Ward, N. A. B., Harrington, R. W. *Organometallics* **2011**, *30*, 6010–6016.

(26) (a) Gorin, D. J.; Sherry, B. D.; Toste, F. D. *Chem. Rev*. **2008**, *109*, 3351–3378. (b) Wang, W.; Hammond, G. B.; Xu, B. *J. Am. Chem. Soc*. **2012**, *134*, 5697–5705.

(27) (a) Pattenden, G. J. Heterocycl. Chem. **1992**, 29, 607-618. (b) Palmer, D. C.; Venkatraman, S. In The Chemistry of Heterocyclic Compounds, A Series of Monographs, Oxazoles: Synthesis, reactions and Spectroscopy, Part A, Ed. Palmer, D. C. John Wiley, Hoboken, 2003.

(28) For isochromenes see: (a) Mondal, S.; Nogami, T.; Asao, N.; Yamamoto, Y. *J. Org. Chem*. **2003**, *68*, 9496–6498. (b) Rosenbaum, D. M.; Cherezov, V.; Hanson, M. A.; Rasmussen S. G. F.; Thian, F. S.; Kobilka, T. S.; Choi, H.; Yao, X.; Weis, W. I.; Stevens, R. C.; Kobilka, B. K. *Science* **2007**, *318*, 1266–1273. (c) Takeuchi, T.; Oishi, S.; Watanabe, T.; Ohno, H.; Sawada, J. I.; Matsumo, K.; Asai, A.; Asada, N.; Kitaura, K.; Fijii, N. *J. Med. Chem*. **2011**, *54*, 4839–4846. (d) Obika, S.; Kono, H.; Yasui, Y.; Yanada, R.; Takemoto, Y. *J. Org. Chem.* **2007**, *72*, 4462–4468. (e) Yue, D.; Della, Ca, N.; Larock, R. C. *Org. Lett*. **2004**, *6*, 1581–1584. (f) Kang, H.-S.; Jun, E.-M.; Park, S.-H.; Heo, S.-J.; Lee, T.-S.; Yoo, I.-D.; Kim, J.-P.; *J. Nat. Prod.* **2007**, *70*, 1043–1045. (g) Mo, S.; Zhou, G.; Yang, Y.; Li, Y.; Chen, X.; Shi, J. *J. Nat. Prod*. **2004**, *67*, 823–828. (h) Zhang, P.; Cyriac, G.; Kopajtic, T.;Zhao, Y.; Javitch, J. A.; Katz, J. L.; Newman, A. H. *J. Med. Chem.* **2010**, *53*, 6112–6121. (i) Wang, W.; Li, T.; Milburn, R.; Yates, J.; Hinnant, E.; Luzzio, M. J.; Noble, S. A.; Attardo, G. Bioorg. *Med. Chem. Lett.* **1998**, *8*. 1579–1584. For iminoisocoumarins see: (j) Soulie, P.; Gamelin, E.; Eder, J. *Proc. Amer. Soc. Clin. Oncol*. 2003, Abstract No. 777. (k) Kawano, T.; Agata, N.; Kharbanda, D.; Avigan, D.; Kufe, D. *Cancer Chemother. Pharmacol*. **2007**, *59*, 329–335.

(29) (a) Marchal, E.; Uriac, P.; Legouin, B.; Toupet, L.; van de Weghe, P. T*etrahedron* **2007**, *63*, 9979–9990. (b) Hashmi, A. S. K.; Schafer, S.; Wolfe, M.; Diez Gil, C.; Fischer, P.; Laguna, A.; Blanco, M. C.; Gimeno, M. C. *Angew. Chem. Int. Ed*. **2007**, *46*, 6184.

(30) (a) Corriu, R. J. P.; Guerin, C.; Henner, B. J. L.; Jolivet, A. *J. Organomet. Chem*. **1997**, *530*, 39–48. (b) Pellizzaro, L.; Fabris, F.; Lucchi, O. De.; Tatibouet, A.; Rollin, P. *Tet. Lett*. **2009**, *50*, 101–103. (c) Kondoh, A.; Yorimitsu, H.; Oshima, K. *J. Am. Chem. Soc*. **2007**, *129*, 4099–4104.

(31) (a) Spek, A. L. *Acta. Cryst*. **1987**, *C43*, 1233–1235. (b) Ruban, G.; Zabel, V. *Cryst. Struct. Commun*. **1076**, *6*, 671–674. (c) Bandoli, D.; Bortolozzo, G.; Clemente, D. A.; Croatto, U. Panattoni, C. *J. Chem. Soc. A*. **1970**, 2778–2780.

(32) (a) Al-Sa′ady, A. K.; McAuliffe, C. A.; Parish R. V.; Sandbank, J. A.; *Inorg. Synth*. **1985**, *23*, 191–194. (b) Baddley, W. H.; Basolo, F.; Gray, H. B.; Nölting, C.; Poë, A. J. *Inorg. Chem*. **1963**, *2*, 921–928. (c) Berners-Price, S. J.; Sadler, P. J. *Inorg. Chem*. **1986**, *25*, 3822–3827.

(33) (a) Herrero-Gómez, E.; Nieto-Oberhuber, C.; López, S.; Benet-Buchholz, J.; Echavarren, A. M. *Angew. Chem. Int. Ed*. **2006**, *45*, 5455–5469. (b) Perez-Galan, P.; Delpont, N.; Herrero-Gomez, E.; Maseras, F.; Echavarren, A. M. *Chem. Eur. J*. **2010**, *16*, 532–5332.

(34) (a) K. N. Kouroulis, K. N.; Hadjikakou, S. K.; Kourkoumelis, N.; Kubicki, M.; Male, L.; Hursthouse, M.; Skoulika, S.; Metsios, A. K.; Tyurin, V. Y.; Dolganov, A. V.; Milaeva, E. R.; Hadjiliadis, N. *Dalton Trans*. **2009**, 1044–10456. (b) Dunstan, S. P. C.; Healy, P. C.; Sobolev, A. N.; Tiekink, E. R. T.; White, A. H.; Williams, M. L. *J. Mol. Struct*. **2014**, *253*, 253–259. (c) Khan, M.; Oldham, C.; Tuck, D. G. *Can. J. Chem*. **1981**, *59*, 2714-2178. (d) Borissova, A. O.; Korlyukov, A. A.; Antipin, M. Y.; Lyssenko, K. A. *J. Phys. Chem A*. **2008**, *112*, 11519–11522.

(35) N. C. Baenziger, W. E. Bennett and D. M. Soborofe, *Acta Crystallogr. Sect. B: Struct. Crystallogr*. *Cryst. Chem*. **1976,** *32*, 962–963.

(36) (a) Partyka, D. V.; Robilotto, T. J.; Zeller, M.; Hunter, A. D.; Gray, T. G. *Organometallics* **2008**, *27*, 28–32. (b) For a recent relevant review that discusses weak gold-arene interaction see: Schmidbaur, H.; Schier, A. *Organometallics* **2010**, *29*, 2–23.

(37) Johnson, C.E.; Bovey, F.A. *J. Chem. Phys.* **1958**, *29*, 1012–1014.

(38) (a) Malhorta, D.; Mashuta, M. S.; Hammond, G. B.; Xu, B. *Angew. Chem. Int. Ed*. **2014**, *53*, 4456–4459. (b) Wang, W.; Hammond, G. B.; Xu, B. *J. Am. Chem. Soc*. **2012**, *134*, 5697–5705.

(39) For a comprehensive and detailed feature article see: (a) Clavier, H.; Nolan, S. P. *Chem. Commun*. **2010**, *46*, 841–861. See also (b) Hillier, A. C.; Sommer, W. J.; Yong, B. S.; Petersen, J. L.; Cavello, L.; Nolan, S. P. *Organometallics*, **2003**, *22*, 4322–4326.

(40) Tolman, C. A. *Chem. Rev*. **1977**, *77*, 313–348.

(41) Poater, A.; Cosenza, B.; Correa, A.; Giudice, S.; Ragone, F.; Scarano, V.; Cavello, L. *Eur. J. Inorg. Chem*. **2009**, 1759–1766. The *SambVca* software is available on-line at: http://www.molnac.unisa.it/OMtools/sambvca.php.

(42) Alyea, E. C.; Ferguson, G.; Gallagher, J.; Malito, J. *Acta. Crystallogr., Sect. C: Cryst. Struct. Commun*. 1**993**, *49*, 1473–1476.

(43) Alyea, E. C.; Ferguson, G.; Kannan, S. *Polyhedron* **2000**, *19*, 2211–2213.

(44) Bott, R. C.; Healy, P. C.; Smith, G. *Aust. J. Chem*. **200**4, *57*, 213–218.

(45) Chen. H. W.; Tiekink, E. R. T. *Acta. Crystallogr., Sect. E*: *Struct. Rep*. Online **2003**, *59*, m50–m51.

(46) Muller, T. E.; Green, J. C.; Mingos, D. M. P. McPartlin, C. M. Wittingham, C.; Williams, D. J. Woodroffe, *J. Organomet. Chem*. **1998**, *551*, 313–330.

(47) Nieger, M.; Niecke, E.; Dany, S. Z. *Kristallogr*. **1997**, 2*12*, 249–250.

(48) (a) Guzei, I. A.; Wendt, M. *Dalton Trans*. **2006**, 3991–3999. (b) Guzei, A. I.; Wendt, M. Program Solid –G, Madison, WI, USA, 2004.

(49) For a comprehensive insight into ligand effects in homogeneous gold(I) catalysis see: (a) Wang, W.; Hammond, G. B.; Xu, B. *J. Am. Chem. Soc*. **2012**, 13*4*, 5697–5705. (b) Li, Q,-S.; Wand, C.-Q.; Zou, R.-Y.; Xu, F.-B.; Song, H.-B.; Wan, X.-J.; Zhang, Z.-Z.; *Inorg. Chem*. **2006**, *45*, 1888–1890.

(50) (a) Brown, T. J.; Weber, D.; Gagné, M. R.; Widenhoefer, R. A. *J. Am. Chem. Soc*. **2012**, *134*, 9134–9137.

(51) For a selection of recent examples see: (a) Chioua, M.; Samadi, A.; Soriano, E.; Infantes, L.; Marco-Contelles, J. *Adv. Synth. C*atal. **2014**, *356*, 1235–1241. (b) Terada, M.; Li, F,; Toda, Y. *Angew. Chem. Int. Ed.* **2014**, *53*, 235–239. (c) Dell′Acqua, M.; Castano, B.; Cecchini, C.; Pedrazzini, T.; Pirovano, V.; Rossi, E.; Caselli, A.; Abbiati, G. *J. Org. Chem*. **2014**, *79*, 3494–3505. (d) Liu, J.; Xie, X.; Liu, Y. *Chem. Commun*. 2**013**, *49*, 11794–11796. (e) Mariaule, G.; Newsome, G.; Toullec, P. Y.; Belmont, P.; Michelet, V. *Org. Lett*. **2014**, *16*, 4570–4573. (f) Su, Y.; Lu, M.; Dong, B.; Chen, H.; Shi, X. Adv. *Synth. Catal*. **2014**, 3*56*, 692–696.

(52) (a) Weber, D.; Gagné, M. R *Org. Lett*. **2009**, *11*, 4962–4965. (b) Homs, A.; Escofet, I.; Echavarren, A. M. *Org. Lett*. **2013**, 1*5*, 5782-5785. (c) Zhu, Y.; Day, C. S.; Zhang, L.; Hauser, K. J.; Jones, A. C. *Chem. Eur*. *J*. **2013**, 19, 12264–12271.

(53) (a) Becker, J. J.; White, P. S.; Gagné, M. R.; *J. Am. Chem. Soc*. **2001**, *123*, 9478–9479. (b) Doherty, S.; Knight, J. G.; Smyth, C. E.; Harington, R. W.; Clegg, W. J. *Org. Chem.* **2006**, *71*, 9751–9764. (c) Doherty, S.; Knight, J. G.; Smyth, C. E.; Harington, R. W.; Clegg, W. O*rganometallics* **2007**, *26*, 5961–5966. (d) Doherty, S.; Knight, J. G.; Smyth, C. E.; Harington, R. W.; Clegg, W. O*rganometallics* **2007**, 2*6*, 6453–6461.

(54) Evans, D. A.; Tregany, S. W.; Burgey, C. S.; Paras, N. A.; Vojkovsky, T. J. *Am. Chem. Soc.* **2000**, 12*2*, 7936–7943.

(55) Hashmi, A. S. K.; Schäfer, S.; Wölfle, M.; Diez Gil, C.; Fischer, P.; Laguna, A.; Blanco, M. C.; Gimeno, M. C. *Angew. Chem. Int. Ed*. **2007**, *46*, 6184–6187.

(56) Li, X.; Chianese, A. R.; Vogel, T.; Crabtree, R. H. *Org. Lett.* **2005**, *7*, 5437–5450.

(57) Lu, D.; Zhou, Y.; Li, Y.; Yan, S.; Gong, Y. *J. Org. Chem.* **2011**, *76*, 8869–8878.

(58) (a) Yu, X.; Ding, Q.; Wang, W.; Wu, J. *Tetrahedron Lett*. **2008**, *49*, 4390–4393. (b) Enomoto, T.; Girard, A.-L.; Takemoto, Y.; Yasui, Y. *J. Org. Chem.* **2009**, *74*, 9158–9164. (c) Obika, S.; Kono, H.; Yasui, Y.; Yanada, R.; Takemoto, Y. *J. Org. Chem.* **2007**, *72*, 4462–4468.

(59) Naoe, S.; Saito, T.; Uchiyama, M.; Oishi, S.; Fujii, N.; Ohno, H. *Org. Lett*. **2015**, *17*, 1774–-1777.

(60) Hashmi, A. S. K. *Chem. Rev*. **2007**, *107*, 3180–3211. (b) Jimenez-Núñez, E.; Echavarren, A. *Chem. Commun*, **2007**, 333–346.

(61) (a) Wilckens, K.; Uhlemann, M.; Czekelius, C. *Chem. Eur. J*. **2009**, *15*, 13323–13326. (b) Wilckens, K.; Lentz, D.; Czekelius, C. *Organometallics* **2011**, *30*, 1287–1290. (c) Bera, M.; Roy, S. *J. Org. Chem.* **2009**, *74*, 8814–8817. (d) Tsukano, C.; Yokouchi, S.; Girard, A.-L.; Kuribayashi, T.; Sakamoto, S.; Enomoto, T.; Takemoto, Y. *Org. Biomol. Chem*. **2012**, *10*, 6074–6086. (e) Zhang, L.; Ye, D.; Liu, G.; Feng, E.; Jiang, H.; Liu, H. *J. Org. Chem.* 2**010**, *75*, 3671–3677. (f) Girard, A.; Enomoto, T.; Yokouchi, T.; Tsukano, C.; Takemoto, T. *Chem. Asian J*. **2011**, *6*, 1321–1324. (g) Yu, Y.; Stephenson, A.; Mitchell, D. *Tetrahedron Lett*. **2006**, *47*, 3811–3814. (h) Ochida, A.; Ito, H.; Sawamura, M. *J. Am. Chem. Soc*. **2006**, *128*, 16486–16487. (i) Iwai, T.; Okochi, H.; Ito, H.; Sawamura, M. *Angew. Chem. Int. Ed*. **2013**, *52*, 4239–4242.

(62) (a) Bellina, F.; Ciucci, D.; Vergamini, P.; Rossi, R. *Tetrahedron* **2000**, *56*, 2533–2545. (b) Marchal, E.; Uriac, P.; Legouin, B.; Toupet, L.; van de Weghe, P. *Tetrahedron* **2007**, *63*, 9979–9990. (c) Genin, E.; Toullec, P. Y.; Antoniotti, S.; Brancour, C.; Genêt, J.-P.; Michelet, V. *J. Am. Chem. Soc*. **2006**, *128*, 3112–3113. (d) Sashida, H.; Kawamukai, A. *Synthesis* **1999**, 1145–1148.

(63) (a) Bian, M.; Yao, W.; Ding, H.; Ma, C. *J. Org. Chem*. **2010**, *75*, 269-272. (b) Liu, G.; Zhou, Y.; Ye, D.; Zhang, D.; Ding, X.; Jiang, H.; Liu, H. *Adv. Synth. Catal.* **2009**, *351*, 2605-2610.

(64) Chary, R. G.; Dhamanjaya, G.; Prasad, K. V.; Vaishaly, S.; Ganesh, Y. S. S.; Dulla, B.; Kumar, K. S.; Pal, M. *Chem. Commun*. **2014**, *50*, 6797-6800.

Insert Table of Contents artwork here